



MHD FLOW OF A NANOFLUID AT THE FORWARD STAGNATION POINT OF AN INFINITE PERMEABLE WALL WITH A CONVECTIVE BOUNDARY CONDITION

Siti Hidayah Muhad Saleh^{1†} — Norihan Md Arifin² — Roslinda Mohd Nazar³ — Ioan Pop⁴

¹Department of Mathematics, Faculty of Science, Universiti Putra Malaysia, 43400 UPM Serdang, Selangor, Malaysia

²Institute For Mathematical Research, Universiti Putra Malaysia, 43400 UPM Serdang, Selangor, Malaysia; Department of Mathematics, Faculty of S. Universiti Putra Malaysia, 43400 UPM Serdang, Selangor, Malaysia

³School of Mathematical Sciences, Faculty of Science and Technology, Universiti Kebangsaan Malaysia, 43600 UKM Bangi, Selangor, Malaysia

⁴Department of Mathematics, Babeş-Bolyai University, R-400084 Cluj-Napoca, Romania

ABSTRACT

The steady magnetohydrodynamic (MHD) flow of a nanofluid at the forward stagnation point of an infinite permeable wall is investigated in this study. A mathematical model has been constructed and the governing partial differential equations are converted into ordinary differential equations by similarity transformation. The similarity equations are solved numerically by a shooting technique. Results for the surface shear stresses, surface heat transfer, and velocity, nanoparticle fraction and temperature profiles are presented in tables and in some graphs. Effects of the magnetic parameter, constant mass flux Biot number, Brownian motion parameter, thermophoresis parameter and Lewis number are examined. The present results are compared with previously available numerical results obtained using other methods of solution, and they are found to be in good agreement.

Keywords: MHD flow, Nanofluid, Stagnation point, Infinite permeable wall, Numerical solution.

Received: 17 May 2016 / Revised: 15 June 2016 / Accepted: 20 September 2016 / Published: 2 November 2016

Contribution/ Originality

This study documents important features of MHD stagnation point flow with the effect of convective boundary condition also suction and injection. The paper's contribution is finding that the development of skin friction, heat flux and mass flux, with the velocity, temperature and nanoparticle fraction profiles, in tables and graphs.

Nomenclature

a	constant
B_0	magnetic field normal to the wall
Bi	Biot number
C	constant nanoparticle fraction
C_f	skin friction coefficient

C_p	specific heat at constant pressure
C_w	constant wall nanoparticle fraction
C_∞	constant nanoparticle fraction (inviscid flow)
D_B	Brownian diffusion coefficient
D_T	thermophoresis diffusion coefficient
h_f	convective heat transfer coefficient
k	thermal conductivity
Le	Lewis number
M	magnetic parameter
Nb	Brownian motion parameter
Nt	thermophoresis parameter
Nu_x	local Nusselt number
Pr	Prandtl number
q_m	mass flux
q_w	heat flux
Re_x	local Reynolds number
s	constant mass flux
Sh_x	local Sherwood number
T	constant temperature
T_f	convective fluid temperature below the surface of the wall
T_w	temperature of the surface of the wall
T_∞	constant temperature (inviscid flow)
u, v	velocity component in the x and y direction, respectively
u_e	external stream (inviscid flow)
v_w	mass flux velocity
x, y	Cartesian coordinates along the surface and normal to it, respectively

α	thermal diffusivity
η	pseudo-similarity variable
ϕ	solid volume fraction of the nanofluid
ρ	density
σ	electric conductivity
θ	dimensionless temperature
τ	ratio between the effective heat capacity of nanoparticle and heat capacity of the fluid
τ_w	skin friction or shear stress
ν	kinematic viscosity
ψ	stream function
$(\rho C_p)_f$	heat capacity of the fluid
$(\rho C_p)_p$	heat capacity of the nanoparticle material

Superscript

'	differentiation with respect to η
---	--

Subscript

w	condition at the wall
∞	condition at infinity

1. INTRODUCTION

The flow near the stagnation point has attracted the attention of many investigators for many years because of its wide applications both in industrial and scientific applications. Some of the applications are cooling of electronic devices by fans, solar central receivers exposed to wind currents, and many hydrodynamic processes in engineering applications. The study of two dimensional stagnation point flows towards a solid surface in moving fluid was first studied by [Hiemenz \[1\]](#) in 1911 and follows by [Homann \[2\]](#) for the axisymmetric stagnation point flow. Many researchers have been working still on the stagnation point flows in various way. [Mahapatra and Gupta \[3\]](#) extended the stagnation point study by considering a stretching surface. Moreover, the stagnation point flow of a micropolar fluid towards stretching sheet was studied by [Nazar \[4\]](#) etc.

The problem of MHD flow at the stagnation point is a thoroughly researched problem in fluid mechanics. The steady MHD mixed convection flow near the stagnation point on a vertical permeable surface has been examined by [Ishak \[5\]](#) and they found that dual solutions are exist for both assisting and opposing cases. [Mahapatra, et al. \[6\]](#); [Ray Mahapatra, et al. \[7\]](#) investigated two dimensional MHD stagnation point flow of a power law fluid towards a stretching surface numerically and analytically.

In recent years, some interest has been given to the study of convective transport of nanofluids. The theory of nanofluid first introduced by [Choi and Eastman \[8\]](#) and has been a field of very active research area. [Kuznetsov and Nield \[9\]](#) examined the influence of nanoparticles on natural convection flow past a vertical flat plate, using a model in which Brownian motion and thermophoresis are accounted for. They found that the reduced Nusselt

number is a decreasing function of Brownian motion and thermophoresis parameter. Then, Khan and Pop [10] formulated the problem of laminar boundary layer flow of a nanofluid past a stretching sheet and Mustafa [11] considering the flow at the stagnation point for nanofluid towards a stretching sheet. The problem of boundary layer flow of a nanofluid past a stretching sheet has been investigated analytically by using the Homotopy Analysis Method by Hassani [12]. This work was extended by Bachok, et al. [13] by taking an account of shrinking case and discover a non-unique solution. Further, they continue the research by considering an unsteady flow and permeable sheet (see Bachok, et al. [14]). Ibrahim, et al. [15] analyzed the effect of magnetic field on stagnation point flow and heat transfer due to nanofluid towards a stretching sheet. There are many other studies have been conducted which relates to nanofluids such as Khan and Aziz [16]; Alsaedi, et al. [17]; Aziz and Khan [18]; Hamad and Ferdows [19] and Rana and Bhargava [20].

There has been considerable interest also in flows past permeable walls with suction and injection. The process of suction and injection has its importance in many engineering applications such as in the design of thrust bearing and radial diffusers, and thermal oil recovery. Suction is applied to chemical processes to remove reactants while injection is used to add reactants, cool the surfaces, prevent corrosion or scaling and reduce the drag (see Labropulu, et al. [21]). Katagiri [22] investigated the behavior of magnetohydrodynamic flow with suction or injection at the forward stagnation point and solved numerically. Kandasamy, et al. [23] explored the problem of MHD boundary layer flow of a nanofluid past a vertical stretching surface in the presence of suction and injection. Then, Ibrahim and Shankar [24] extended the study by took into account the slip boundary condition past a permeable stretching sheet. The same boundary layer flow of nanofluid also been investigated for semi infinite flat plate by Hamad, et al. [25]. Recently, the influenced of nanoparticles on mixed convection boundary layer flow along an inclined surface in a porous medium with Brownian motion and thermophoresis effect were examined by Rana, et al. [26]. The similarity solutions to the convective heat transfer problems have been studied by Aziz [27] and Magyari [28] for an impermeable plate, and by Ishak [29] for a permeable plate.

Recently, there are studies of heat transfer problem for boundary layer flow that put convective boundary condition into account. Aziz [27] discussed on the similarity solution of thermal boundary layer over a flat plate and then Ishak [29] extends it by considering the effect of suction and injection. The effect of convective boundary condition in nanofluid also have been investigated by Makinde, et al. [30] with internal heat generation/absorption and followed by Alsaedi, et al. [17] with analysis of stagnation point flow. An effect of stretching and shrinking with convective boundary condition was analyzed by Bachok, et al. [31] and Nandy and Mahapatra [32]. Recently, Akbar [33] and Hamad, et al. [34] conducted a study of MHD stagnation point flow under convective boundary condition with radiation effects. It is worth mentioning that many other boundary layer problems with convective boundary condition were investigated by Merkin and Pop [35]; Rashad, et al. [36]; Makinde and Aziz [37]; Makinde and Aziz [38] and Makinde, et al. [39].

Motivated by the above investigations, the present paper deals with the problem of steady MHD boundary layer flow and heat transfer and nanoparticle fraction over a two-dimensional stagnation point on an infinite permeable wall with convective boundary condition. We also investigate the effect of suction and injection on the system. The governing partial differential equations are first transformed into ordinary differential equations using similarity transformation, before being solved numerically by using shooting technique. The numerical results obtained are then compared with the data available in the literature for certain particular cases of the problem, to support their validity.

2. BASIC EQUATIONS

Consider the steady two-dimensional laminar flow of an incompressible and viscous nanofluid at the forward stagnation point of an infinite permeable wall, which is assumed to be an electric insulator. It is assumed that the velocity of the external stream (inviscid flow) is $u_e(x) = ax$, where a is a positive the constant, and v_w is the mass flux velocity, where $v_w < 0$ corresponds to suction and $v_w > 0$ corresponds to injection, respectively. Then, we assume that the constant temperature T and the constant nanoparticle fraction C in the ambient fluid (inviscid flow) are denoted by T_∞ and C_∞ , respectively. A uniform magnetic field B_0 is applied normal to the wall. The nanofluid is assumed to have constant properties. In addition, the assumptions of small magnetic Reynolds number and of zero electric field have been made. Cartesian coordinates x and y are measured along the wall and perpendicular to it, respectively, as shown in Figure 1.

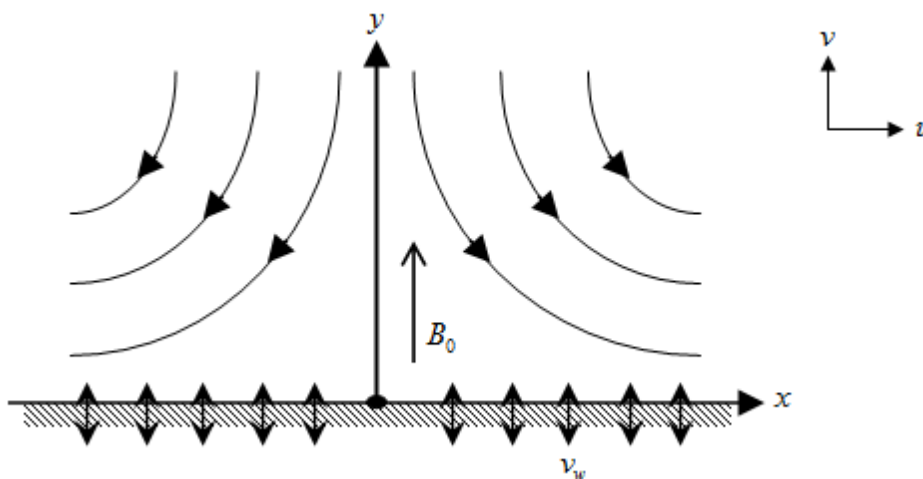


Figure-1. Physical model and coordinate system

Under these assumptions, the basic boundary layer equations of conservation of mass, momentum, thermal energy and nanoparticle fraction can be written as, see [Kuznetsov and Nield \[9\]](#) and [Katagiri \[22\]](#).

$$\frac{\partial u}{\partial x} + \frac{\partial v}{\partial y} = 0 \tag{1}$$

$$u \frac{\partial u}{\partial x} + v \frac{\partial u}{\partial y} = u_e \frac{d u_e}{d x} + \nu \frac{\partial^2 u}{\partial y^2} + \frac{\sigma B_0^2}{\rho} (u_e - u) \tag{2}$$

$$u \frac{\partial T}{\partial x} + v \frac{\partial T}{\partial y} = \alpha \frac{\partial^2 T}{\partial y^2} + \tau \left[D_B \frac{\partial T}{\partial y} \frac{\partial C}{\partial y} + \frac{D_T}{T_\infty} \left(\frac{\partial T}{\partial y} \right)^2 \right] \tag{3}$$

$$u \frac{\partial C}{\partial x} + v \frac{\partial C}{\partial y} = D_B \frac{\partial^2 C}{\partial y^2} + \frac{D_T}{T_\infty} \frac{\partial^2 T}{\partial y^2} \tag{4}$$

where u and v are the velocity component in the x and y directions, ν is the kinematic viscosity, α is the thermal diffusivity of the nanofluid, ρ is the density, σ is the electric conductivity, D_B is the Brownian diffusion

coefficient, D_T is the thermophoresis diffusion coefficient and τ is the ratio between the effective heat capacity of the nanoparticle material and heat capacity of the fluid, $\tau = (\rho C_p)_p / (\rho C_p)_f$, C_p being the specific heat at constant pressure.

Following Aziz [27] and Ishak [29] we assume that the temperature of the surface of the wall is maintained by convective heat transfer at a certain value T_w , which is to be determined later. Thus, the boundary conditions of Eqs. (1) - (4) are

$$v = v_w, \quad u = 0, \quad -k \frac{\partial T}{\partial y} = h_f (T_f - T_w), \quad C = C_w \quad \text{at} \quad y = 0$$

$$u \rightarrow u_e, \quad T \rightarrow T_\infty, \quad C \rightarrow C_\infty \quad \text{as} \quad y \rightarrow \infty$$
(5)

Where k is the thermal conductivity, T_f is the convective fluid temperature below the surface of the wall, h_f is the convective heat transfer coefficient and C_w is the constant wall nanoparticle fraction.

We look for a similarity solution of Eqs. (1) to (4), with the boundary conditions (5) of the following form

$$\psi = (\nu a)^{1/2} x f(\eta), \quad \theta(\eta) = \frac{T - T_\infty}{T_w - T_\infty}, \quad \phi(\eta) = \frac{C - C_\infty}{C_w - C_\infty}, \quad \eta = \left(\frac{a}{\nu}\right)^{1/2} y$$
(6)

where ψ is the stream function, which is defined as $u = \partial\psi/\partial y$ and $v = -\partial\psi/\partial x$. Thus, we have

$$u = ax f'(\eta), \quad v = -(a\nu)^{1/2} f(\eta)$$
(7)

where primes denote differentiation with respect to η . Therefore, in order that Eqs. (1) - (4) have a similarity solution, we take

$$v_w = -(a\nu)^{1/2} s$$
(8)

where s is the constant mass flux where $s > 0$ corresponds for suction and $s < 0$ correspond for injection, respectively.

Substituting (7) into Eqs.(2) to (4), we obtain the following ordinary differential equations

$$f''' + f f'' + 1 - f'^2 + M(1 - f') = 0$$
(9)

$$\frac{1}{Pr} \theta'' + f \theta' + Nb \theta' \phi' + Nt (\theta')^2 = 0$$
(10)

$$\phi'' + Le f \phi' + \frac{Nt}{Nb} \theta'' = 0$$
(11)

and the boundary conditions (5) become

$$f(0) = s, \quad f'(0) = 0, \quad \theta'(0) = -Bi[1 - \theta(0)], \quad \phi(0) = 1$$

$$f'(\eta) \rightarrow 1, \quad \theta(\eta) \rightarrow 0, \quad \phi(\eta) \rightarrow 0 \quad \text{as} \quad \eta \rightarrow \infty$$
(12)

Where $Pr = \nu/\alpha$ is the Prandtl number and $Le = \nu/D_B$ is the Lewis number. Further, M is the magnetic parameter, Bi is the Biot number, Nb is the Brownian motion parameter and Nt is the thermophoresis parameter, which are defined as

$$M = \frac{\sigma B_0^2}{\rho a}, \quad Bi = \frac{h_f}{k} \left(\frac{a}{\nu} \right)^{1/2}, \quad Nb = \frac{\tau D_B (C_w - C_\infty)}{\nu}, \quad Nt = \frac{\tau D_T (T_w - T_\infty)}{\nu T_\infty} \tag{13}$$

Quantities of physical interest are the skin friction coefficients C_f , the local Nusselt number Nu_x and the local Sherwood number Sh_x , which can be expressed as

$$C_f = \frac{\tau_w}{\rho u_e^2}, \quad Nu_x = \frac{x q_w}{k(T_w - T_\infty)}, \quad Sh_x = \frac{x q_m}{D_B (C_w - C_\infty)} \tag{14}$$

where τ_w is the skin friction or shear stress and, q_w and q_m are the heat flux and the mass flux, respectively, from the surface of the sheet, which are defined as

$$\tau_w = -\mu \left(\frac{\partial u}{\partial y} \right)_{y=0}, \quad q_w = -k \left(\frac{\partial T}{\partial y} \right)_{y=0}, \quad q_m = -D_B \left(\frac{\partial C}{\partial y} \right)_{y=0} \tag{15}$$

Substituting (6) into (15) and using (14), we obtain

$$Re_x^{1/2} C_f = f''(0), \quad Re_x^{-1/2} Nu_x = -\theta'(0), \quad Re_x^{-1/2} Sh_x = -\phi'(0) \tag{16}$$

where $Re_x = u_e(x)x/\nu$ is the local Reynolds numbers.

It is worth mentioning that when $Bi = 0$, the lower side of the wall with hot fluid is totally insulated and no convective heat transfer to the cold fluid upwards of the wall takes place. Further, it should be noticed at this end that the solution of the energy equation (10) approaches the solution of the constant surface temperature $\theta(0) = 1$ as $Bi \rightarrow \infty$.

3. RESULTS AND DISCUSSION

The ordinary differential equations (9) to (11) subject to the boundary condition (12) have been solved numerically for some values of the governing parameters M, s, Bi, Nb, Nt and Le using a shooting method. The value of the Prandtl number is taken $Pr = 1$ throughout this paper. In addition, we also interested to look on some physical quantities which were skin friction coefficient, $f''(0)$, the heat flux $-\theta'(0)$ and mass flux $-\phi'(0)$.

The obtained results for the skin friction coefficient $f''(0)$, for various values of the parameter M and s have been compared with those reported by Katagiri [22] and were shown in Table 1. Note that this is for the case of no energy and no concentration equation. From this table, we noticed that the comparison shows a very good agreement for each value of $f''(0)$, $-\theta'(0)$ and $-\phi'(0)$. This comparison lends confidence in the numerical

results to be reported in the next table for several values of Le and Bi for both suction and injection cases. By referring Table 2, it shows that the values of $f''(0)$ were independent of Le and Bi . The values of $-\theta'(0)$ and $-\phi'(0)$ decrease as Le and Bi increase except for $-\phi'(0)$ in suction case where it increase when Le increase.

Fig. 2 shows the effects of s and M on $f''(0)$ graphically. From this figure, it shows that as both parameter M and s increase, the values of $f''(0)$ also increase. The same results also have been agreed by Katagiri [22] for impermeable case. From Fig. 3, as Nt increase from 0 to 0.6, the values of $-\theta'(0)$ decrease for both suction and injection cases. Similar result have been observed by Aziz and Khan [18]. The graph also illustrate that when Nb increase, $-\theta'(0)$ decrease for both suction and injection cases. The variation of $-\phi'(0)$ as Nt increase have been shown at Fig. 4. We can see clear difference for both suction and injection cases where along with an increment of Nt value, the value of $-\phi'(0)$ decrease for suction case but increase for injection case. The graph also explain the changes of $-\phi'(0)$ as Nb increase. From Fig. 4(a), we noticed that the value of $-\phi'(0)$ increase when Nb increase while $-\phi'(0)$ decrease when Nb increase for injection case which shown at Fig. 4(b).

Next, we can see the variation of $-\phi'(0)$ for different values of Lewis number, Le and Biot number, Bi from Fig. 5. The value of $-\phi'(0)$ increase for suction case while decrease for injection case when the value of Lewis number, Le increase. Fig. 5 (a) illustrate that $-\phi'(0)$ was slightly decrease at the beginning as Bi increase. Whilst, a slight increase of $-\phi'(0)$ at $Bi < 1$ can be seen in Fig. 5(b) when Bi increase.

Fig. 6 to 9 illustrate the effects of parameter M , s , Nb and Bi on velocity profile $f'(\eta)$, temperature profile $\theta(\eta)$ and nanoparticle fraction profiles $\phi(\eta)$. These profiles satisfy the far field boundary conditions (12) asymptotically, which support the validity of numerical solution obtained. For Fig. 6, it shows the effects of M on each profiles where the solid line refers to suction case and broken line refers to injection case. By referring to Fig. 6(a), when the value of M increase, the velocity also increase for both suction and injection cases. Fig. 6(b) explains that the temperature of the system decrease when M increase. The same trend can be found in Fig. 6(c), where the nanoparticle fraction decrease when M increase for both cases. In addition, we also can see that there are small influence of M on temperature and nanoparticle profiles for suction case compared to injection case by referring on Fig. 6(b) and (c).

Fig. 7 shows the effects of S on each profiles. From Fig. 7(a), it explained that the velocity of the system are increase together with S which also obtained by Katagiri [22] for impermeable case. However, contrary to the present observation, Ishak [5] and Bachok, et al. [14] found that as s increase, the velocity decrease for regular fluid and nanofluid, respectively. Besides, the temperature and nanoparticle fraction are decreased with S which can be seen in Fig. 8(b) and (c), and Bachok, et al. [14] also reported the similar result. We also noticed that the graph shape is still the same from the value of suction to injection.

Fig. 8 illustrate the temperature profiles with the change of Brownion motion parameter, Nb . From Fig. 8 (a), it shows that the temperature increase with Nb for both suction and injection cases. A slight different of trend can be seen for nanoparticle fraction when suction and injection (see Fig. 8(b)). For suction case, we can see that nanoparticle fraction decrease when Nb increase.

Effects of Biot number Bi on temperature profiles can be seen in Fig. 9. It shows that both temperature for suction and injection cases are increase together with the value of Bi . Furthermore, the higher the Bi , the closer the value of $\theta(0)$ approaching 1 at the boundary. This can be proved from the boundary condition (12)

which reduces to $\theta(0) = 1$ if $Bi \rightarrow \infty$. Aziz [27] noted the same pattern for the temperature profiles.

Table-1. Comparison of results for the values of $f''(0)$ for several values of M and S .

M	S	Katagiri [22] $f''(0)$	Present Results
			$f''(0)$
1	-1	1.116421	1.116421
	-0.5	1.331153	1.331154
	0	1.585327	1.585331
	0.5	1.877166	1.877176
	1	2.20292	2.202940
	1.5	2.557898	2.557937
	2	2.937316	2.937384
	2.5	3.336797	3.336905
	3	3.752586	3.752749
2	-1	1.405659	1.405659
	-0.5	1.622920	1.622924
	0	1.873519	1.873527
	0.5	2.156606	2.156623
	1	2.469924	2.469955
	1.5	2.810327	2.810379
	2	3.174309	3.174391
	2.5	3.558404	3.558527
	3	3.959429	3.959605

Table-2. Values of $f''(0)$, $-\theta'(0)$ and $-\phi'(0)$ for several values of Bi when $M = 1$, $S = 1$ (suction), $S = -1$

(injection) and $Pr = 1$.

S	Le	Bi	$f''(0)$	$-\theta'(0)$	$-\phi'(0)$
1	1	0.1	2.202940	0.910438	1.275161
		0.5	2.202940	0.661393	1.113066
		1.0	2.202940	0.487094	1.010323
		5.0	2.202940	0.152556	0.836141
		10.0	2.202940	0.081723	0.802935

	5	0.1	2.202940	0.897044	5.195860
		0.5	2.202940	0.621653	5.073030
		1.0	2.202940	0.441633	5.005761
		5.0	2.202940	0.129098	4.910766
		10.0	2.202940	0.068203	4.895214
	10	0.1	2.202940	0.893047	10.11542
		0.5	2.202940	0.610363	10.00105
		1.0	2.202940	0.429316	9.941435
		5.0	2.202940	0.12335	9.86200
		10.0	2.202940	0.064957	9.849624
-1	1	0.1	1.116421	0.490115	0.189373
		0.5	1.116421	0.151282	0.222413
		1.0	1.116421	0.080664	0.229284
		5.0	1.116421	0.017009	0.235469
		10.0	1.116421	0.008562	0.236289
	5	0.1	1.116421	0.482957	0.017123
		0.5	1.116421	0.147208	0.024405
		1.0	1.116421	0.078291	0.025803
		5.0	1.116421	0.016472	0.027030
		10.0	1.116421	0.008289	0.027191
	10	0.1	1.116421	0.482478	0.005580
		0.5	1.116421	0.146969	0.008633
		1.0	1.116421	0.078156	0.009209
		5.0	1.116421	0.016442	0.009713
		10.0	1.116421	0.008274	0.009779

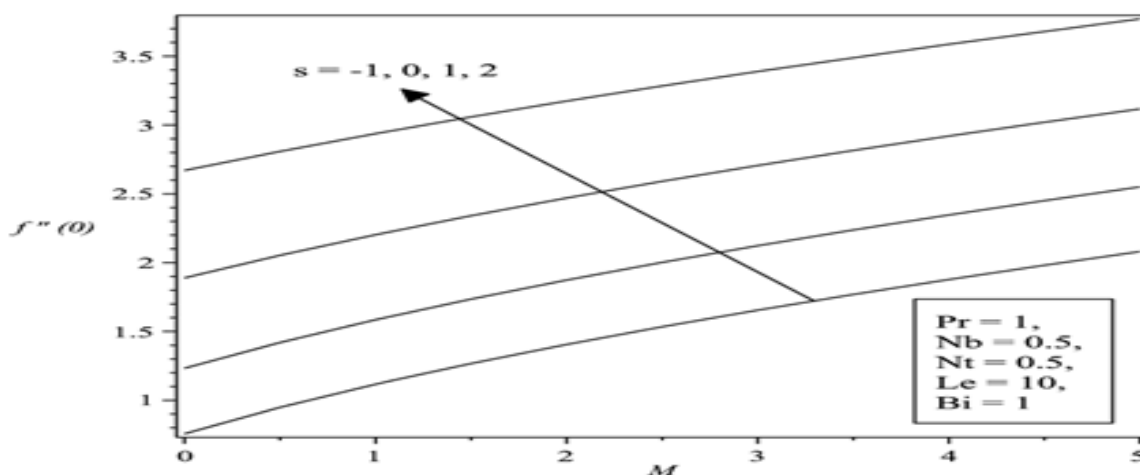


Fig-2. Variation of $f''(0)$ with M for several values of s when $Nb = 0.5$, $Nt = 0.5$, $Le = 10$ and $Bi = 1$.

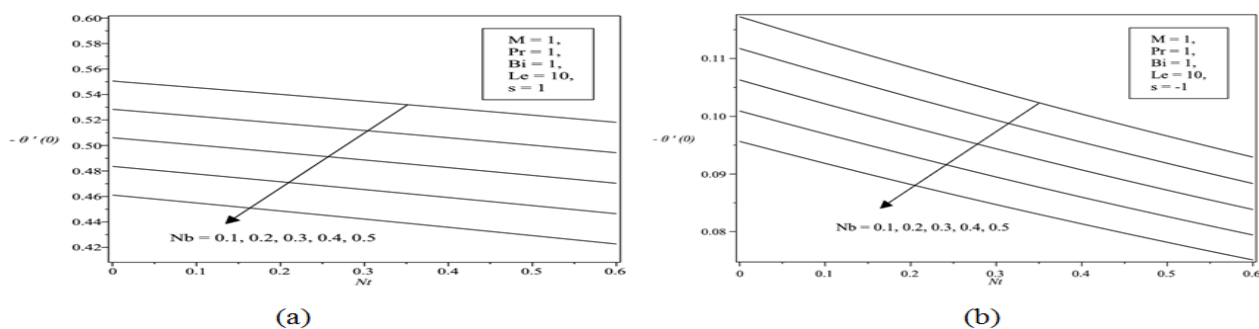


Fig-3. Variation of $-\theta'(0)$ with Nt for several values of Nb when $M = 1$, $Le = 10$ and $Bi = 1$ for (a) suction and (b) injection case

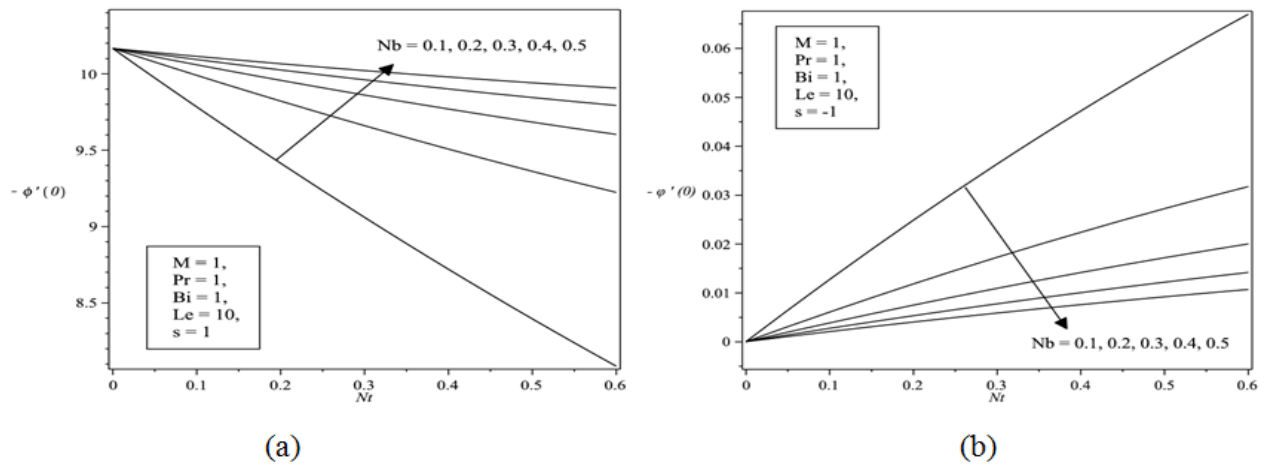


Fig-4. Variation of $-\phi'(0)$ with Nt for several values of Nb when $M = 1, Le = 10$ and $Bi = 1$ for (a) suction and (b) injection case

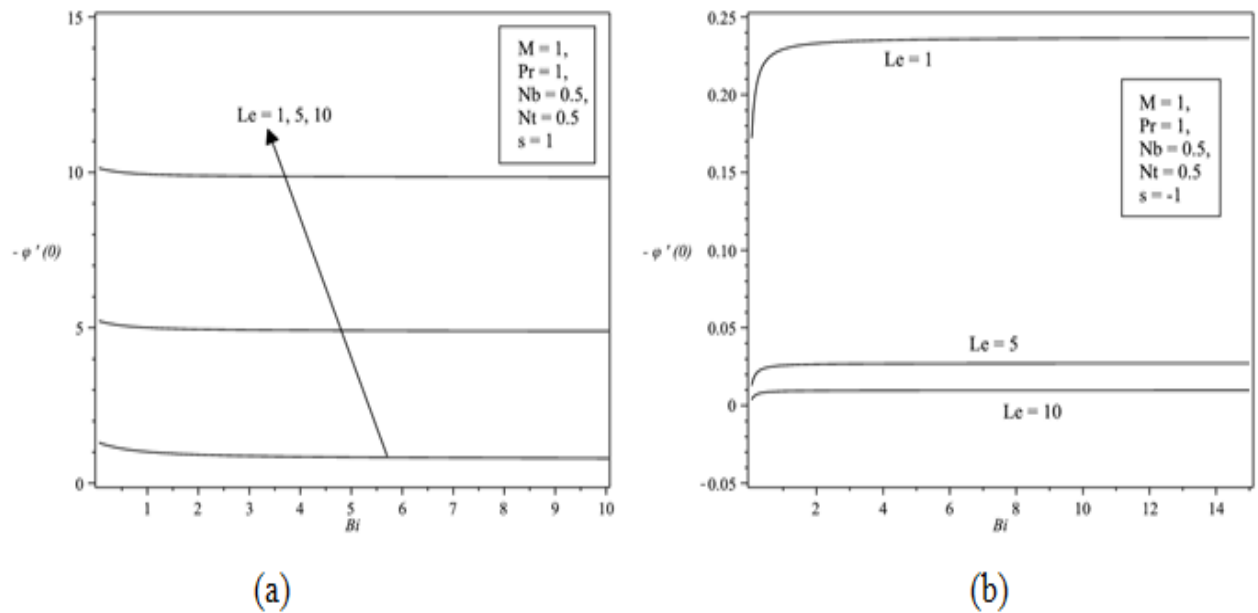


Fig-5. Variation of $-\phi'(0)$ with Bi for several values of Le when $M = 1, Nb = 0.5, Nt = 0.5$ and $Bi = 1$ for (a) suction and (b) injection case

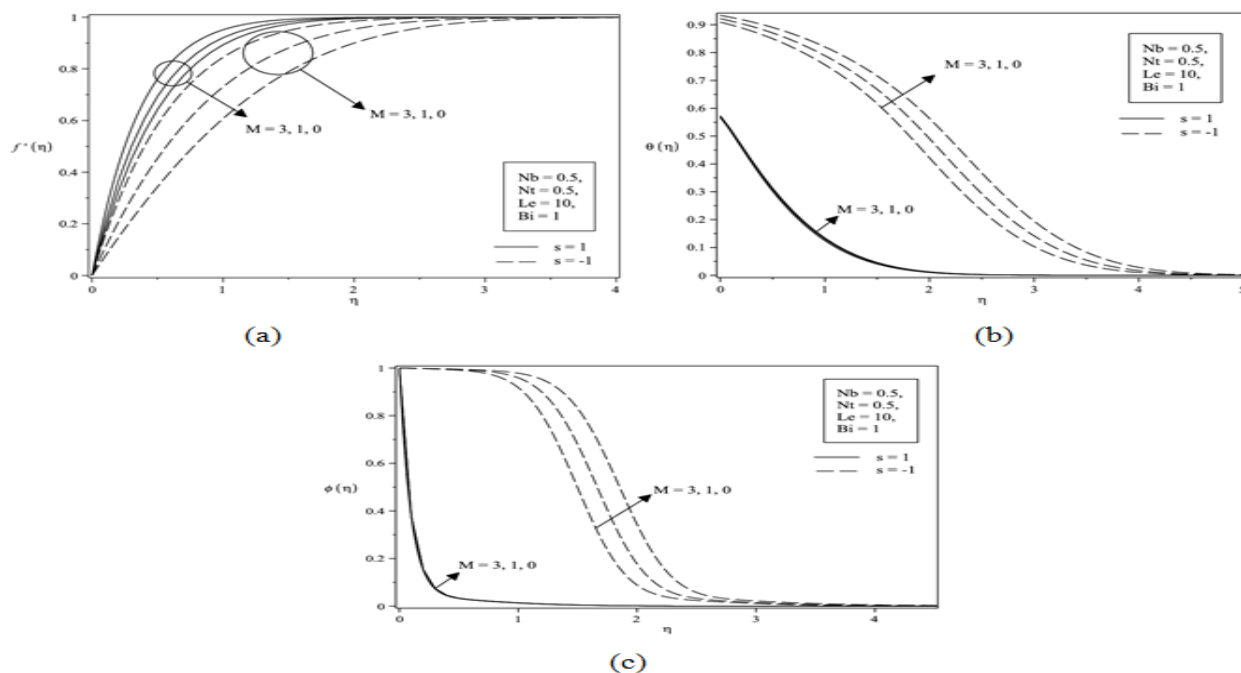


Fig-6. Effects of M on the (a) velocity profile $f'(\eta)$, (b) temperature profile $\theta(\eta)$ and (c) nanoparticle fraction profiles $\phi(\eta)$ when $Nb = 0.5$, $Nt = 0.5$, $Le = 10$ and $Bi = 1$ for both suction ($s = 1$) and injection ($s = -1$) cases.

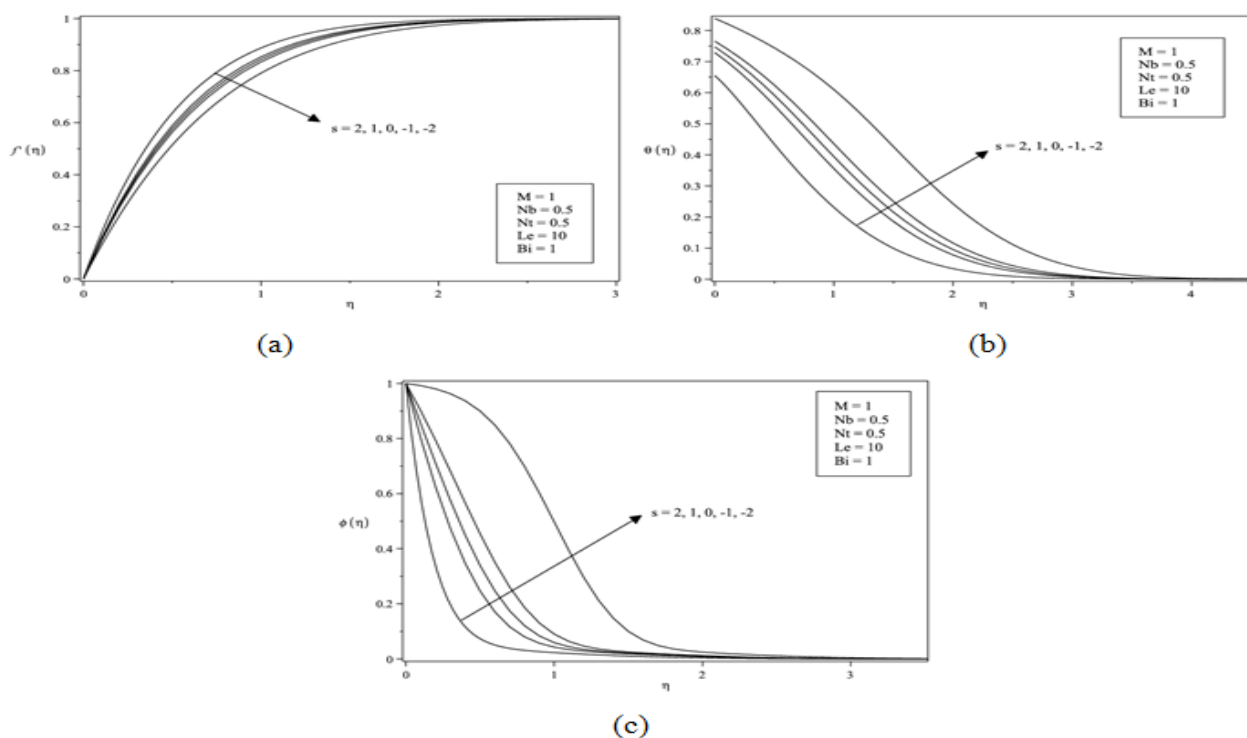


Fig-7. Effects of S on the (a) velocity profile $f'(\eta)$, (b) temperature profile $\theta(\eta)$ and (c) nanoparticle fraction profiles $\phi(\eta)$ when $Nb = 0.5$, $Nt = 0.5$, $Le = 10$ and $Bi = 1$.

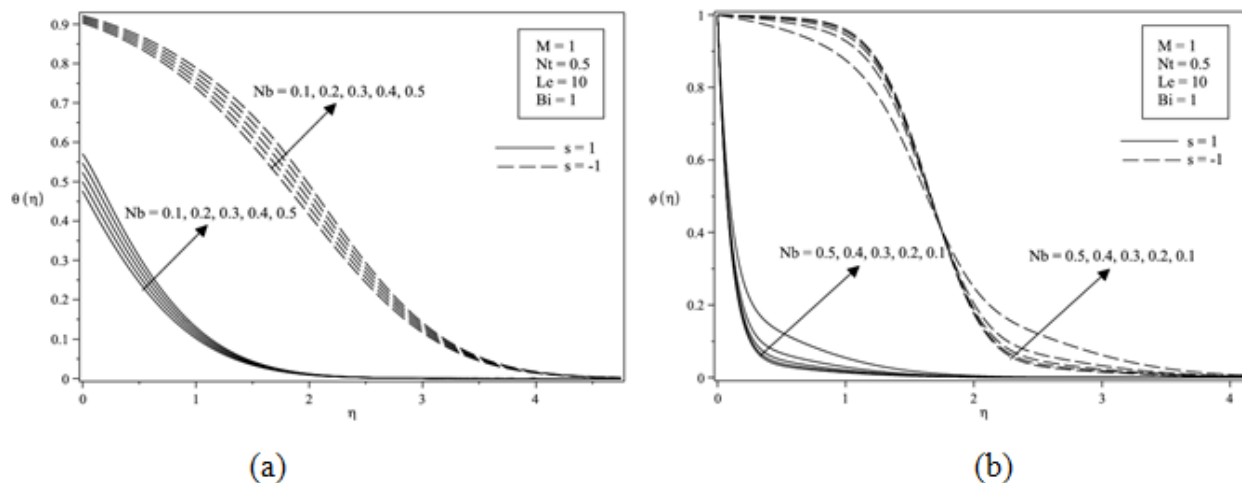


Fig-8. Effects of Nb on the (a) temperature profile $\theta(\eta)$ and (b) nanoparticle fraction profiles $\phi(\eta)$ when $M = 1$, $Nt = 0.5$, $Le = 10$ and $Bi = 1$ for both suction ($s = 1$) and injection ($s = -1$) cases.

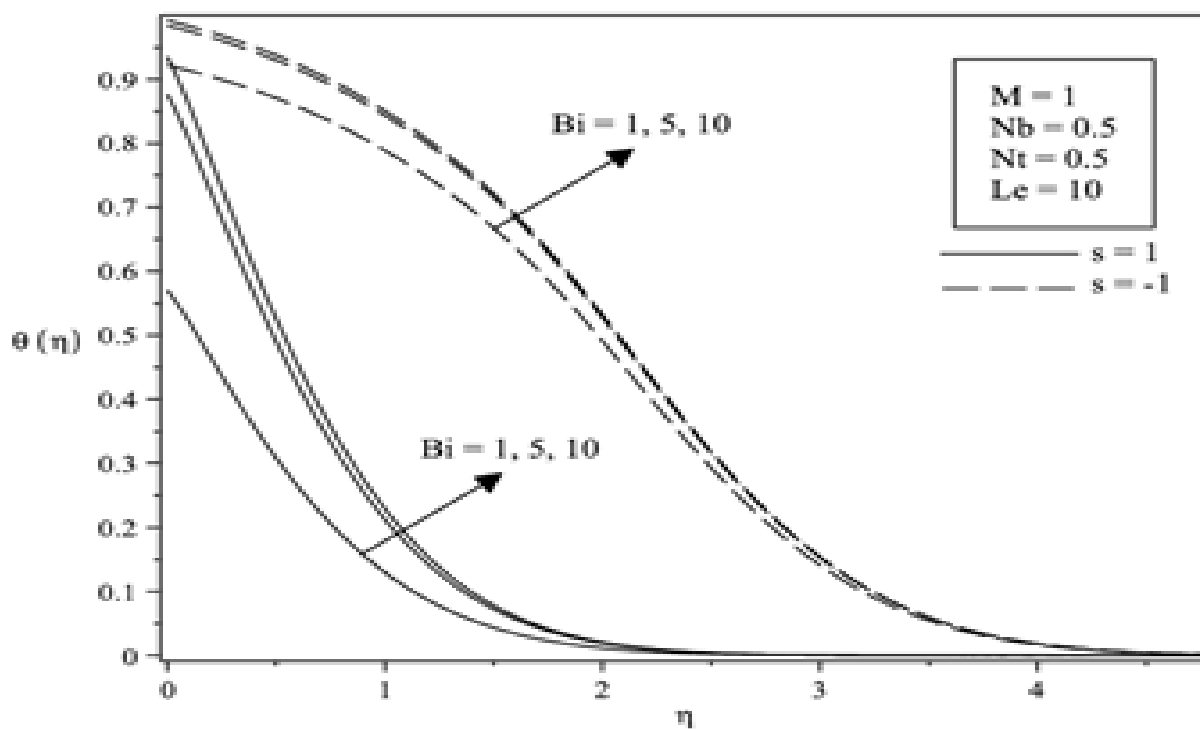


Fig-9. Effects of Bi on the temperature profile $\theta(\eta)$ when $M = 1$, $Nt = 0.5$, $Nb = 0.5$ and $Le = 10$ for both suction ($s = 1$) and injection ($s = -1$) cases.

4. CONCLUSION

We have theoretically investigated the effects of various governing parameters magnetic parameter M , constant suction/injection parameter s , Brownian motion parameter Nb , thermophoresis parameter Nt , Biot number Bi and Lewis number Le on flow field and heat transfer characteristics of the MHD stagnation point flow of a nanofluid at the forward stagnation point of an infinite permeable wall. The numerical results obtained are in excellent agreement with the previously published data available. It is found that the magnitude of skin friction

$f''(0)$, the local Nusselt number $-\theta'(0)$ and the local Sherwood number $-\phi'(0)$ all are increasing with M and s .

Funding: This study received no specific financial support.

Competing Interests: The authors declare that they have no competing interests.

Contributors/Acknowledgement: All authors contributed equally to the conception and design of the study. The authors gratefully acknowledge the financial supports received in the form of research grant fund from the Ministry of Higher Education, Malaysia.

REFERENCES

- [1] K. Hiemenz, *Die Grenzschicht an einem in den gleichförmigen Flüssigkeitsstrom eingetauchten geraden Kreiszylinder*. Berlin: Weber, 1911.
- [2] F. Homann, "Der Einfluß großer Zähigkeit bei der Strömung um den Zylinder und um die Kugel," *ZAMM - Journal of Applied Mathematics and Mechanics / Zeitschrift für Angewandte Mathematik und Mechanik*, vol. 16, pp. 153-164, 1936.
- [3] T. R. Mahapatra and A. S. Gupta, "Stagnation-point flow towards a stretching surface," *Canadian Journal of Chemical Engineering*, vol. 81, pp. 258-263, 2003.
- [4] R. Nazar, "Stagnation point flow of a micropolar fluid towards a stretching sheet," *International Journal of Non-Linear Mechanics*, vol. 39, pp. 1227-1235, 2004.
- [5] A. Ishak, "MHD mixed convection flow near the stagnation-point on a vertical permeable surface," *Physica A: Statistical Mechanics and its Applications*, vol. 389, pp. 40-46, 2010.
- [6] T. R. Mahapatra, S. K. Nandy, and A. S. Gupta, "Analytical solution of magnetohydrodynamic stagnation-point flow of a power-law fluid towards a stretching surface," *Applied Mathematics and Computation*, vol. 215, pp. 1696-1710, 2009.
- [7] T. Ray Mahapatra, S. K. Nandy, and A. S. Gupta, "Magnetohydrodynamic stagnation-point flow of a power-law fluid towards a stretching surface," *International Journal of Non-Linear Mechanics*, vol. 44, pp. 124-129, 2009.
- [8] S. U. S. Choi and J. A. Eastman, *Enhancing thermal conductivity of fluids with nanoparticles*. Medium: ED; Size, n.d.
- [9] A. V. Kuznetsov and D. A. Nield, "Natural convective boundary-layer flow of a nanofluid past a vertical plate," *International Journal of Thermal Sciences*, vol. 49, pp. 243-247, 2010.
- [10] W. A. Khan and I. Pop, "Boundary-layer flow of a nanofluid past a stretching sheet," *International Journal of Heat and Mass Transfer*, vol. 53, pp. 2477-2483, 2010.
- [11] M. Mustafa, "Stagnation-point flow of a nanofluid towards a stretching sheet," *International Journal of Heat and Mass Transfer*, vol. 54, pp. 5588-5594, 2011.
- [12] M. Hassani, "An analytical solution for boundary layer flow of a nanofluid past a stretching sheet," *International Journal of Thermal Sciences*, vol. 50, pp. 2256-2263, 2011.
- [13] N. Bachok, A. Ishak, and I. Pop, "Stagnation-point flow over a stretching/shrinking sheet in a nanofluid," *Nanoscale Research Letters*, vol. 6, pp. 1-10, 2011.
- [14] N. Bachok, A. Ishak, and I. Pop, "Unsteady boundary-layer flow and heat transfer of a nanofluid over a permeable stretching/shrinking sheet," *International Journal of Heat and Mass Transfer*, vol. 55, pp. 2102-2109, 2012.
- [15] W. Ibrahim, B. Shankar, and M. M. Nandeppanavar, "MHD stagnation point flow and heat transfer due to nanofluid towards a stretching sheet," *International Journal of Heat and Mass Transfer*, vol. 56, pp. 1-9, 2013.
- [16] W. A. Khan and A. Aziz, "Natural convection flow of a nanofluid over a vertical plate with uniform surface heat flux," *International Journal of Thermal Sciences*, vol. 50, pp. 1207-1214, 2011.

- [17] A. Alsaedi, M. Awais, and T. Hayat, "Effects of heat generation/absorption on stagnation point flow of nanofluid over a surface with convective boundary conditions," *Communications in Nonlinear Science and Numerical Simulation*, vol. 17, pp. 4210-4223, 2012.
- [18] A. Aziz and W. A. Khan, "Natural convective boundary layer flow of a nanofluid past a convectively heated vertical plate," *International Journal of Thermal Sciences*, vol. 52, pp. 83-90, 2012.
- [19] M. A. A. Hamad and M. Ferdows, "Similarity solution of boundary layer stagnation-point flow towards a heated porous stretching sheet saturated with a nanofluid with heat absorption/generation and suction/blowing: A lie group analysis," *Communications in Nonlinear Science and Numerical Simulation*, vol. 17, pp. 132-140, 2012.
- [20] P. Rana and R. Bhargava, "Flow and heat transfer of a nanofluid over a nonlinearly stretching sheet: A numerical study," *Communications in Nonlinear Science and Numerical Simulation*, vol. 17, pp. 212-226, 2012.
- [21] F. Labropulu, J. M. Dorrepaal, and O. P. Chandna, "Oblique flow impinging on a wall with suction or blowing," *Acta. Mechanica*, vol. 115, pp. 15-25, 1996.
- [22] M. Katagiri, "Magnetohydrodynamic flow with suction or injection at the forward stagnation point," *Journal of the Physical Society of Japan*, vol. 27, pp. 1677-1685, 1969.
- [23] R. Kandasamy, K. Gunasekaran, and S. b. H. Hasan, "Scaling group transformation on fluid flow with variable stream conditions," *International Journal of Non-Linear Mechanics*, vol. 46, pp. 976-985, 2011.
- [24] W. Ibrahim and B. Shankar, "MHD boundary layer flow and heat transfer of a nanofluid past a permeable stretching sheet with velocity, thermal and solutal slip boundary conditions," *Computers & Fluids*, vol. 75, pp. 1-10, 2013.
- [25] M. A. A. Hamad, I. Pop, and A. I. Md Ismail, "Magnetic field effects on free convection flow of a nanofluid past a vertical semi-infinite flat plate," *Nonlinear Analysis: Real World Applications*, vol. 12, pp. 1338-1346, 2011.
- [26] P. Rana, R. Bhargava, and O. A. Bég, "Numerical solution for mixed convection boundary layer flow of a nanofluid along an inclined plate embedded in a porous medium," *Computers & Mathematics with Applications*, vol. 64, pp. 2816-2832, 2012.
- [27] A. Aziz, "A similarity solution for laminar thermal boundary layer over a flat plate with a convective surface boundary condition," *Communications in Nonlinear Science and Numerical Simulation*, vol. 14, pp. 1064-1068, 2009.
- [28] E. Magyari, "The moving plate thermometer," *International Journal of Thermal Sciences*, vol. 47, pp. 1436-1441, 2008.
- [29] A. Ishak, "Similarity solutions for flow and heat transfer over a permeable surface with convective boundary condition," *Applied Mathematics and Computation*, vol. 217, pp. 837-842, 2010.
- [30] O. D. Makinde, W. A. Khan, and Z. H. Khan, "Buoyancy effects on MHD stagnation point flow and heat transfer of a nanofluid past a convectively heated stretching/shrinking sheet," *International Journal of Heat and Mass Transfer*, vol. 62, pp. 526-533, 2013.
- [31] N. Bachok, A. Ishak, and I. Pop, "Stagnation point flow toward a stretching/shrinking sheet with a convective surface boundary condition," *Journal of the Franklin Institute*, vol. 350, pp. 2736-2744, 2013.
- [32] S. K. Nandy and T. R. Mahapatra, "Effects of slip and heat generation/absorption on MHD stagnation flow of nanofluid past a stretching/shrinking surface with convective boundary conditions," *International Journal of Heat and Mass Transfer*, vol. 64, pp. 1091-1100, 2013.
- [33] N. S. Akbar, "Radiation effects on MHD stagnation point flow of nano fluid towards a stretching surface with convective boundary condition," *Chinese Journal of Aeronautics*, vol. 26, pp. 1389-1397, 2013.
- [34] M. A. A. Hamad, M. J. Uddin, and A. I. M. Ismail, "Radiation effects on heat and mass transfer in MHD stagnation-point flow over a permeable flat plate with thermal convective surface boundary condition, temperature dependent viscosity and thermal conductivity," *Nuclear Engineering and Design*, vol. 242, pp. 194-200, 2012.
- [35] J. H. Merkin and I. Pop, "The forced convection flow of a uniform stream over a flat surface with a convective surface boundary condition," *Communications in Nonlinear Science and Numerical Simulation*, vol. 16, pp. 3602-3609, 2011.

- [36] A. M. Rashad, A. J. Chamkha, and M. Modather, "Mixed convection boundary-layer flow past a horizontal circular cylinder embedded in a porous medium filled with a nanofluid under convective boundary condition," *Computers & Fluids*, vol. 86, pp. 380-388, 2013.
- [37] O. D. Makinde and A. Aziz, "MHD mixed convection from a vertical plate embedded in a porous medium with a convective boundary condition," *International Journal of Thermal Sciences*, vol. 49, pp. 1813-1820, 2010.
- [38] O. D. Makinde and A. Aziz, "Boundary layer flow of a nanofluid past a stretching sheet with a convective boundary condition," *International Journal of Thermal Sciences*, vol. 50, pp. 1326-1332, 2011.
- [39] O. D. Makinde, T. Chinyoka, and L. Rundora, "Unsteady flow of a reactive variable viscosity non-Newtonian fluid through a porous saturated medium with asymmetric convective boundary conditions," *Computers & Mathematics with Applications*, vol. 62, pp. 3343-3352, 2011.

Views and opinions expressed in this article are the views and opinions of the author(s), International Journal of Mathematical Research shall not be responsible or answerable for any loss, damage or liability etc. caused in relation to/arising out of the use of the content.